arXiv:cond-mat/9909364v1 [cond-mat.mtrl-sci] 24 Sep 1999

Simulations of metastable decay in two- and three-dimensional models with microscopic dynamics

M.A. Novotny[a,0], P.A. Rikvold[a,b,0],
M. Kolesik[c], D.M. Townsley[a,b,1], R.A. Ramos[d]

[a]Supercomputer Computations Research Institute,
Florida State University, Tallahassee, FL 32306-4130, USA

[b]Center for Materials Research and Technology and Department of Physics,
Florida State University, Tallahassee, FL 32306-4350, USA

[c]Department of Mathematics, University of Arizona, Tucson, AZ 85721, USA

[d]Department of Physics, University of Puerto Rico, Mayaguez, PR 00681, USA

February 1, 2008

Abstract

We present a brief analysis of the crossover phase diagram for the decay of a metastable phase in a simple dynamic lattice-gas model of a two-phase system. We illustrate the nucleation-theoretical analysis with dynamic Monte Carlo simulations of a kinetic Ising lattice gas on square and cubic lattices. We predict several regimes in which the metastable lifetime has different functional forms, and provide estimates for the crossovers between the different regimes. In the multidroplet regime, the Kolmogorov-Johnson-Mehl-Avrami theory for the time dependence of the order-parameter decay and the two-point density correlation function allows extraction of both the order parameter in the metastable phase and the interfacial velocity from the simulation data.

1999 PACS numbers: 64.60.My, 64.60.Qb, 81.30.-t, 05.50.+q

[0] Corresponding authors. Fax: +1-850-644-0098; e-mails: novotny@scri.fsu.edu, rikvold@scri.fsu.edu
[1] Present address: Department of Physics, University of California, Santa Barbara, CA 93106-9530, USA.

1 Introduction

The decay of a metastable phase through nucleation and growth of droplets of a more stable phase is a common feature of phase-transformation processes in both natural and technological settings. It occurs both in systems where the phases involved are non-crystalline and crystalline [1]. Often such processes are well described by a combination of nucleation theory [2] and the Kolmogorov-Johnson-Mehl-Avrami (KJMA) theory [3, 4, 5], which describes nucleation followed by irreversible growth of the nucleated droplets [6].

Here we present some recent theoretical results on the effects of finite system size in simple model systems with microscopic dynamics, which undergo decay of a metastable phase through homogeneous nucleation and growth. These results are illustrated and confirmed by extensive dynamic Monte Carlo (MC) simulations. The simulations utilize several advanced algorithms [7, 8, 9, 10, 11] that enable numerical study of extremely long-lived metastable phases *without* changing the underlying dynamics. Although the models that we study are highly simplified, there is evidence from magnetic systems that the predicted finite-size effects are experimentally observable [12, 13]. Moreover, our data-analysis methods should also be applicable to experiments.

The rest of this paper is organized as follows. The theoretical model is presented in Sec. 2, and relevant aspects of the nucleation and KJMA theories are presented in Sec. 3. Results of MC simulations are given in Sec. 4. In particular, we present a "metastability phase diagram," metastable lifetimes for two- and three-dimensional systems, and measurements of the metastable order parameter and the propagation velocities of domain walls in two-dimensional systems. A discussion and conclusions are given in Sec. 5.

2 Theoretical Model

We consider a simple lattice-gas model of a two-phase system, defined by the effective Hamiltonian

$$\mathcal{H}_{\mathrm{LG}} = -\phi \sum_{\langle i,j \rangle} c_i c_j - \mu \sum_i c_i \ . \tag{1}$$

Here $c_i \in \{0,1\}$ is a local concentration variable at the ith site of a d-dimensional hypercubic lattice with periodic boundary conditions, ϕ is an attractive interaction between neighboring sites, and μ is a chemical potential favoring $c_i=1$. The sums $\sum_{\langle i,j \rangle}$ and $\sum_i$ run over all nearest-neighbor pairs and all lattice sites, respectively, and the lattice constant is taken as unity. The order parameter conjugate to μ is the dimensionless density (for $d = 2$ often called "coverage"), $\theta = \mathcal{N}^{-1} \sum_i c_i$, where $\mathcal{N}$ is the total number of sites. Below a critical temperature T_c, two uniform phases coexist along a line of first-order phase transitions at

$\mu = \mu_0 = -d\phi$. Here μ can be interpreted as an (electro)chemical potential, or related to an (osmotic) pressure p as $\mu - \mu_0 = k_{\rm B}T \ln(p/p_0)$ where $k_{\rm B}$ is Boltzmann's constant, T the absolute temperature, and p_0 the pressure at coexistence. Analogous relations can be made to supersaturation, supercooling, etc. Since the distance of μ from the coexistence curve is the important parameter, we introduce the notation $\Delta\mu = \mu - \mu_0$ [14].

The phase degeneracy that leads to coexistence is lifted for $\Delta\mu \neq 0$. For $\Delta\mu > 0$ the high-density phase with θ near unity is the equilibrium phase, while $\Delta\mu < 0$ favors the low-density phase. In both cases the uniform phase which is not favored by the sign of $\Delta\mu$ can be extremely long-lived. The kinetics of the decay towards equilibrium of a system initially in such a long-lived *metastable* phase is the topic of this paper.

The lattice-gas model does not have an intrinsic dynamic. However, on time scales that are long compared to an inverse phonon frequency, the approach to equilibrium can be described by a stochastic dynamic. Here we study *local* dynamics, in which the density is not conserved. Among the many possible dynamics that satisfy detailed balance, and thus ensure approach to equilibrium, we choose the single-site Glauber dynamic [15] with updates at random sites. In this dynamic a proposed update of a single c_i is accepted with the probability $W(c_i \to 1-c_i) = [1+\exp(\Delta E/k_{\rm B}T)]^{-1}$, where ΔE is the energy change which would ensue if the update were accepted. Each attempted update advances the clock by one step, and we measure time in MC Steps per Site (MCSS).

3 Nucleation and Growth

Next we summarize elements of the theory of phase transformation by nucleation and growth in systems with nonconserved order parameter. For further details, see Refs. [6, 12, 16]. We concentrate on homogeneous nucleation, thus ignoring effects of surfaces or disorder. Hence our comparisons will be with simulations using periodic boundary conditions and position-independent interactions and chemical potentials.

A central role is played by the *metastable lifetime*, $\langle \tau(\Delta\mu, T, L) \rangle$, which is the typical time it takes to convert half of the system volume from the metastable to the stable phase. For concreteness we define it as the mean first-passage time to $\theta = 1/2$ from an initial condition with all $c_i = 1$ and $\Delta\mu < 0$.

For the class of attractive lattice-gas models with short-range interactions studied here, the fluctuations that lead to the decay of the metastable phase are compact, d-dimensional droplets of radius R. The free energy of the droplet has two competing terms: a positive interface term $\propto R^{d-1}$, and a negative bulk term $\propto |\Delta\mu| R^d$. The competition between

these yields a critical droplet radius,

$$R_c(\Delta\mu, T) \approx \frac{(d-1)\sigma(T)}{|\Delta\mu|\Delta\theta_0(T)} \,, \tag{2}$$

where $\sigma(T)$ is the equilibrium surface tension and $\Delta\theta_0(T)$ is the equilibrium density difference at coexistence. Both are positive for $T < T_c$. Droplets with $R < R_c$ tend to decay, while droplets with $R > R_c$ tend to continue growing. The free-energy cost of the critical droplet with $R = R_c$, relative to the uniform metastable phase, is

$$\Delta F(\Delta\mu, T) = \Omega_d \sigma(T)^d \left(\frac{d-1}{|\Delta\mu|\Delta\theta_0(T)} \right)^{d-1} , \tag{3}$$

where Ω_d is a weakly T-dependent shape factor such that the volume of a droplet of radius R is $\Omega_d R^d$. Nucleation is a stochastic process, and the nucleation rate per unit volume is given by a Van't Hoff-Arrhenius relation,

$$I(\Delta\mu, T) \propto |\Delta\mu|^K \exp\left[-\frac{\Xi(T)}{k_{\rm B}T|\Delta\mu|^{d-1}} \right] , \tag{4}$$

where $\Xi(T)$ is the $\Delta\mu$-independent part of ΔF. For the model studied here, the prefactor exponent K equals 3 for $d = 2$ [6, 16, 17, 18] and is believed to be $-1/3$ for $d = 3$ [18].

For systems of finite linear size L, a T- and L-dependent crossover called the Thermodynamic Spinodal (THSP), $|\Delta\mu|_{\rm THSP}$ [16] is determined by the condition $R_c \approx L$. Thus $|\Delta\mu|_{\rm THSP} \sim L^{-1}$. For $|\Delta\mu| < |\Delta\mu|_{\rm THSP}$, R_c would exceed L. This is called the Coexistence (CE) regime because the critical fluctuation here resembles two coexisting domains of different density. For $|\Delta\mu| > |\Delta\mu|_{\rm THSP}$ (but not too large, as discussed below), the lifetime is dominated by the inverse of the total nucleation rate:

$$\langle \tau_{\rm SD}(\Delta\mu, T, L) \rangle \approx \Big(L^d I(\Delta\mu, T) \Big)^{-1} \propto L^{-d} |\Delta\mu|^{-K} \exp\left[\frac{\Xi(T)}{k_{\rm B}T|\Delta\mu|^{d-1}} \right] . \tag{5}$$

This is inversely proportional to the system volume, L^d. The subscript SD stands for Single Droplet and indicates that the phase transformation is completed by the first critical droplet which nucleates.

The fact that a supercritical droplet grows at a finite velocity, $v(\Delta\mu, T)$, leads to a second crossover, called the Dynamic Spinodal (DSP) [16]. A reasonable criterion to locate the DSP is that the average time between nucleation events, $\langle \tau_{\rm SD} \rangle$, should equal the time it takes a droplet to grow to a size comparable to L. This gives the asymptotic relation

$$|\Delta\mu|_{\rm DSP}(T, L) \sim \left[\frac{\Xi(T)}{(d+1)k_{\rm B}T \ln L} \right]^{\frac{1}{d-1}} . \tag{6}$$

The DSP is shown in Fig. 1 for two different values of L. The convergence to zero as $L \to \infty$ is exceedingly slow, so that the crossover is observable in sufficiently small systems [12, 13]. For $|\Delta\mu| > |\Delta\mu|_{\rm DSP}$, the metastable phase decays through many droplets which nucleate and grow independently in different parts of the system. This is called the Multidroplet (MD) regime [16]. The KJMA theory of metastable decay in large systems [3, 4, 5] gives the lifetime in this regime,

$$\langle \tau_{\rm MD}(\Delta\mu, T) \rangle \approx \left[\frac{\Omega_d I v^d}{(d+1)\ln 2} \right]^{-\frac{1}{d+1}} \tag{7}$$

$$\propto v^{\frac{-d}{d+1}} |\Delta\mu|^{\frac{-K}{d+1}} \exp\left[\frac{\Xi(T)}{(d+1) k_{\rm B} T |\Delta\mu|^{d-1}} \right] , \tag{8}$$

which is *independent* of L. Note that the velocity depends on T and $\Delta\mu$. Comparing Eqs. (5) and (8), it becomes clear that it is useful to plot $\ln\langle\tau\rangle$ vs $1/|\Delta\mu|^{d-1}$. In such plots, which are shown in Fig. 2, the lifetimes in both regimes lie on approximately straight lines, with the slope in the SD regime $(d+1)$ times that in the MD regime.

In the MD regime the order parameter decays according to "Avrami's law,"

$$\frac{\langle\theta(t)\rangle - \theta_{\rm s}(\Delta\mu, T)}{\theta_{\rm ms}(\Delta\mu, T) - \theta_{\rm s}(\Delta\mu, T)} \approx \exp\left[-\ln 2 \left(\frac{t}{\langle\tau_{\rm MD}\rangle} \right)^{d+1} \right] , \tag{9}$$

where $\theta_{\rm s}(\Delta\mu, T)$ and $\theta_{\rm ms}(\Delta\mu, T)$ are the equilibrium and quasi-equilibrium values of the density in the stable and metastable phases, respectively. Equilibrium simulations or measurements easily yield $\theta_{\rm s}(\Delta\mu, T)$. By fitting Eq. (9) to simulational or experimental data for $\theta(t)$, one can therefore estimate $\theta_{\rm ms}(\Delta\mu, T)$ and $\langle\tau_{\rm MD}(\Delta\mu, T)\rangle$. The latter gives the combination Iv^d of the nucleation rate and growth velocity [Eq. (7)], but not I and v separately. These quantities can, however, be resolved by using results for the two-point density correlation functions in the KJMA picture [19, 20]. These give the time-dependent variance

$$\langle\theta^2(t)\rangle - \langle\theta(t)\rangle^2 \approx L^{-d} d\Omega_d \left[\langle\theta(t)\rangle - \theta_{\rm s}\right]^2 \Phi(I v^d t^{d+1}) \, (2t)^d \, v^d , \tag{10}$$

where Φ is determined by numerical integration of an expression involving the correlation function [12, 21]. The last factor of v^d in Eq. (10) is not multiplied by I. This permits the separate determination of v by measurement of the variance of $\theta(t)$ in a series of independent simulations or experiments.

The description of the decay in terms of droplets breaks down for sufficiently large $|\Delta\mu|$. The crossover marking the transition to this Strongly Forced (SF) regime is estimated as the L-independent "Mean-Field Spinodal" (MFSP), $|\Delta\mu|_{\rm MFSP}(T)$, for which $R_c = 1/2$.

4 Numerical Results

The "metastability phase diagram" for the square-lattice Ising lattice-gas model is shown in Fig. 1. The three decay regimes shown are the SF, MD, and SD regimes. The CE regime, which occurs at very low $|\Delta\mu|$, is not shown. The MFSP, which separates the SF regime from the other regimes, is given by Eq. (2) with exactly known expressions for both $\sigma(T)$ and $\Delta\theta_0$. This curve goes to zero at T_c. The DSP is shown for two system sizes, L=24 and 240. Our estimate for the location of the DSP is where the standard deviation of the lifetime, $\Delta\tau$, is equal to $\langle\tau\rangle/2$. In the SD (and CE) regimes $\Delta\tau\approx\langle\tau\rangle$, while $\Delta\tau \ll \langle\tau\rangle$ in the MD and SF regimes [16].

As L increases, the portion of the diagram occupied by the MD regime increases. For $2 < 2|\Delta\mu|/\phi < 4$, the critical droplet consists of a single lattice site [22]. For the dynamic used here, there exists an analytical low-temperature estimate for the DSP in this range of $|\Delta\mu|$ [23]. It is obtained by equating the growth time and the nucleation time, and is (for $d = 2$) given by

$$\frac{2|\Delta\mu|_{\rm DSP}(T,L)}{\phi} = 4 - \frac{4k_{\rm B}T}{\phi}\left(\frac{3}{2}\ln L - 0.82\right) \ . \tag{11}$$

The only adjustable parameter is the last term inside the parenthesis, which was fit to give agreement for L between 8 and 240. This expression for the DSP is marked by the two solid straight lines in Fig. 1. It separates the SF regime from a low-temperature SD regime, where the nucleating droplet occupies only a single lattice site. The agreement between the simulation data and the analytical expression is very good. Below the intersection with the MFSP, the low-temperature form for $|\Delta\mu|_{\rm DSP}$ merges smoothly into the form given by Eq. (6), which goes to zero as $T \to T_c$.

As seen from Eqs. (5) and (8), plotting $\langle\tau\rangle$ versus $1/|\Delta\mu|^{d-1}$ gives a reasonable estimate for $\Xi(T)/k_{\rm B}T$ in the SD regime and $\Xi(T)/(d+1)k_{\rm B}T$ in the MD regime. Examples are shown in Fig. 2 for d=2 (a) and d=3 (b). Slight curvatures are present, due to prefactors in the nucleation rate and also to the proximity of a crossover (the THSP, DSP, or MFSP). Well away from crossovers, the curvatures have been used to estimate the prefactor exponent K [6, 16]. The symbols in both panels (with error estimates from $\Delta\tau$), are from 1000 simulations using the n-fold way algorithm [7].

The n-fold way algorithm is based on dividing all sites into classes reflecting the current state of the site and its neighbors. It yields class populations of n=10 classes for d=2 and n=14 classes for d=3. These populations can be utilized to 'coarse-grain' or 'lump' all configurations onto the one-dimensional variable θ. Measuring these class populations and utilizing the analytical form for the acceptance probabilities yields average growth and shrinkage rates for the stable phase. This is the central idea behind the Projective Dynamics

(PD) method [8, 9, 10], which was used to obtain the curves in Fig. 2. Here we measured the class populations in equilibrium, which provides reasonable approximations for the actual class populations during metastable escape for small $|\Delta\mu|$. This approximation causes the slight differences between the curves and the measured data points. Using the correct measured class populations during the escape from the metastable phase gives the exact lifetime (within statistical errors) [10]. The PD method also enables one to obtain results for large systems from class populations in small systems [8, 9]. In fact, the PD results for the large systems in Fig. 2 are obtained from the equilibrium class populations in the smaller systems. By using such advanced algorithms [7, 8, 9, 10, 11], one can speed up calculations of metastable lifetimes by many orders of magnitude — *without* changing the dynamics of the system.

The approximate KJMA theory of phase transformation kinetics is a remarkably versatile tool for analysis of experimental results. Nevertheless, there are very few studies in which it has been explicitly tested in theoretical models with microscopic dynamics on a length scale much smaller than R_c [21, 24, 25]. Here we present results using Eqs. (9) and (10) to analyse the decay of the metastable phase in d=2 MC simulations in the MD regime at $0.8T_c$ [21]. The systems are sufficiently large to contain at least several hundred supercritical droplets (L=256 for $2|\Delta\mu|/\phi > 0.20$ and L=1024 for $0.20 > 2|\Delta\mu|/\phi > 0.12$).

Figure 3 shows the metastable density $\theta_{\rm ms}(\Delta\mu, T)$ for $\Delta\mu < 0$, obtained by fitting data for $\langle\theta(t)\rangle$ to Eq. (9). The equilibrium density $\theta_{\rm s}(\Delta\mu, T)$ is shown for $\Delta\mu \geq 0$. As one would expect, the metastable phase becomes gradually less well defined as $|\Delta\mu|$ is increased. This is reflected by the increasing differences between the data points shown as empty circles and squares, which were obtained using different data cutoffs in the fitting procedure [21]. For smaller $|\Delta\mu|$ these estimates coincide, indicating that the details of the fitting procedure become unimportant as the metastable phase becomes more well defined. As a check on the procedure, metastable densities measured by a transfer-matrix method [21] are also shown. The agreement between the estimates obtained by these two unrelated methods is remarkable over the whole range of $|\Delta\mu|$ shown.

In Fig. 4 we show the average velocity of the convoluted interface between the metastable and stable phases, $v(\Delta\mu, T)$, obtained by fitting Eq. (10) to the variance of the simulated densities, while using the values of $\theta_{\rm ms}$ and Iv^2 obtained from fitting $\langle\theta(t)\rangle$ to Eq. (9). As a check on this rather indirect way of estimating the velocity, the figure also contains data from a simulation of a flat interface propagating into a metastable bulk phase in which nucleation is suppressed [26], and a curve obtained from an analytical nonlinear-response approximation [21, 26]. The agreement between the different estimates is good over the whole range of $|\Delta\mu|$ shown.

5 Discussion and Conclusion

We have shown that even for the simple case of homogeneous nucleation and growth applicable to the decay of the metastable phase in a nearest-neighbor Ising lattice-gas model with periodic boundary conditions, there are different decay regimes separated by crossovers (Fig. 1). This is because there are four length scales in the problem. Two length scales are fixed, the lattice spacing and the linear system size L. Two length scales depend on T and the distance $|\Delta\mu|$ from the coexistence curve. These are the critical droplet radius R_c and the typical size to which a supercritical droplet grows before it interacts with another, $R_0 \approx \langle\tau_{\rm MD}\rangle v$. Starting from the smallest $|\Delta\mu|$, the different decay regimes are the CE regime where $2R_{\rm c} \geq L$, the SD regime where $2R_c \ll L \ll R_0$ and a single nucleating droplet is responsible for the decay of the metastable phase, the MD regime where $R_0 \ll L$ and many supercritical droplets are formed during the decay process, and the SF regime where the droplet picture is not applicable. These regimes are separated by crossover lines, which depend on T and L in different ways. Between the CE and SD regimes is the Thermodynamic Spinodal with $|\Delta\mu|_{\rm THSP} \sim 1/L$. Between the SD and MD regimes is the Dynamic Spinodal with $|\Delta\mu|_{\rm DSP} \sim 1/(\ln L)^{\frac{1}{d-1}}$ asymptotically for *very large* L. Between the MD and SF regimes is the Mean-Field Spinodal, which is independent of L.

The average metastable lifetime $\langle\tau\rangle$ takes different functional forms in the different regimes (Fig. 2). For example, in the SD regime it is inversely proportional to the volume [Eq. (5)], while in the MD regime it is independent of the volume [Eq. (8)]. In the MD regime, "Avrami's law" for the time dependence of the order-parameter decay yields $\theta_{\rm ms}$ and the combination Iv^d of the nucleation rate I and the interface velocity v. However, including two-point density correlation functions enables one to obtain I and v separately. By fitting the KJMA theory to simulation data for d=2 we obtain results for the metastable density (Fig. 3) and interfacial velocity (Fig. 4) that agree with unrelated methods of calculating the same quantities. We believe the data-analysis methods discussed here should be applicable to many experimental systems, as well.

Acknowledgements

We acknowledge comments on the manuscript by G. Brown, G. Korniss, and S. J. Mitchell. This research was supported in part by National Science Foundation Grants No. DMR-9871455 and DMR-9634873 and by Florida State University through the Center for Materials Research and Technology and the Supercomputer Computations Research Institute (U.S. Department of Energy Contract No. DE-FC05-85ER25000).

References

[1] I. Gutzow, J. Schmelzer, A. Dobreva, J. Non-Cryst. Solids 219 (1997) 1; L. Gránásy, P.F. James, J. Non-Cryst. Solids 253 (1999) 210.

[2] F.F. Abraham, Homogeneous Nucleation Theory, Academic, New York, 1974.

[3] A.N. Kolmogorov, Bull. Acad. Sci. USSR, Phys. Ser. 1 (1937) 355.

[4] W.A. Johnson, R.F. Mehl, Trans. Am. Inst. Mining and Metallurgical Engineers 135 (1939) 416.

[5] M. Avrami, J. Chem. Phys. 7 (1939) 1103; 8 (1940) 212; 9 (1941) 177.

[6] P.A. Rikvold, B. M. Gorman, in: D. Stauffer (Ed.), Annual Reviews of Computational Physics I, World Scientific, Singapore, 1994 and references therein.

[7] A.B. Bortz, M.H. Kalos, J. L. Lebowitz, J. Comput. Phys. 17 (1975) 10; M.A. Novotny, Computers in Physics 9 (1995) 46.

[8] M. Kolesik, M.A. Novotny, P.A. Rikvold, D.M. Townsley, in: D.P. Landau, K.K. Mon, B. Schüttler (Eds.), Computer Simulation Studies in Condensed Matter Physics X, Springer, Berlin, 1998.

[9] M. Kolesik, M. Novotny, P.A. Rikvold, Phys. Rev. Lett. 80 (1998) 3384.

[10] M.A. Novotny, M. Kolesik, P.A. Rikvold, Computer Phys. Commun. in press. E-print: cond-mat/9811039.

[11] M.A. Novotny, Phys. Rev. Lett. 74 (1995) 1; erratum 75 (1995) 1424.

[12] H.L. Richards, S.W. Sides, M.A. Novotny, P.A. Rikvold, J. Magn. Magn. Mater. 150 (1995) 37.

[13] P.A. Rikvold, M.A. Novotny, M. Kolesik, H.L. Richards, in: A.T. Skjeltorp, D. Sherrington (Eds.), Dynamical Phenomena in Unconventional Magnetic Systems, Kluwer, Dordrecht, 1998 and references therein.

[14] Equation (1) is equivalent to the ferromagnetic Ising model, $\mathcal{H}_{\rm I} = -J\sum_{\langle i,j\rangle} s_i s_j - H\sum_i s_i$. Thus T_c is known exactly for d=2 and with high numerical precision for d=3. The transformations are: s_i=2c_i−1, J=$\phi/4$, and H=$\Delta\mu/2$. For easy comparison with the Ising literature, $\Delta\mu$ is given in the figures in terms of $2\Delta\mu/\phi{\equiv}H/J$.

[15] K. Binder, D.W. Heermann, Monte Carlo Simulation in Statistical Physics. An Introduction. Third Edition, Springer, Berlin, 1997.

[16] P.A. Rikvold, H. Tomita, S. Miyashita, S.W. Sides, Phys. Rev. E 49 (1994) 5080.

[17] J.S. Langer, Ann. Phys. (N.Y.) 41 (1967) 108; Phys. Rev. Lett. 21 (1968) 973; Ann. Phys. (N.Y.) 54 (1969) 258.

[18] N.J. Günther, D.A. Nicole, D.J. Wallace, J. Phys. A 13 (1980) 1755.

[19] K. Sekimoto, Phys. Lett. A 105 (1984) 390; J. Phys. Soc. Jpn. 53 (1984) 2425; Physica 135A (1986) 328; Int. J. Mod. Phys. B 5 (1991) 1843.

[20] S. Ohta, T. Ohta, K. Kawasaki, Physica 140A (1987) 478.

[21] R.A. Ramos, P.A. Rikvold, M.A. Novotny, Phys. Rev. B 59 (1999) 9053.

[22] E. Jordão Neves, R.H. Schonmann, Commun. Math. Phys. 137 (1991) 209.

[23] J. Lee, M.A. Novotny, P.A. Rikvold, Phys. Rev. E 52 (1995) 356.

[24] K.R. Elder, J.D. Gunton, M. Grant, Phys. Rev. E 54 (1996) 6476.

[25] V.A. Shneidman, K.A. Jackson, K.M. Beatty, Phys. Rev. B 59 (1999) 3579; J. Chem. Phys. 111 (1999) in press.

[26] P.A. Rikvold, M. Kolesik, submitted to J. Stat. Phys. E-print: cond-mat/9909188.

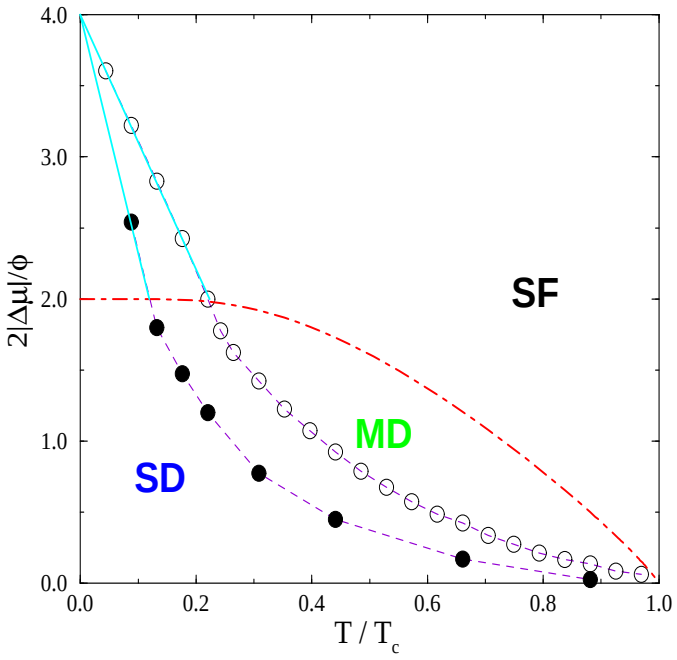

Figure 1: "Metastability phase diagram" for d=2, with the Single Droplet (SD), Multidroplet (MD), and Strongly Forced (SF) regimes labeled. The coexistence (CE) regime for very small $|\Delta\mu|$ is not shown. The dot-dashed line is the estimate for the Mean-Field Spinodal (MFSP), as described in the text. The estimates for the Dynamic Spinodal (DSP) are shown for L=24 (empty circles) and L=240 (filled circles). These data points are joined by dashed lines as guides to the eye, and agree with the analytical low-temperature expression for $2|\Delta\mu|_{\rm DSP}/\phi > 2$ from Eq. (11), marked by the solid straight lines.

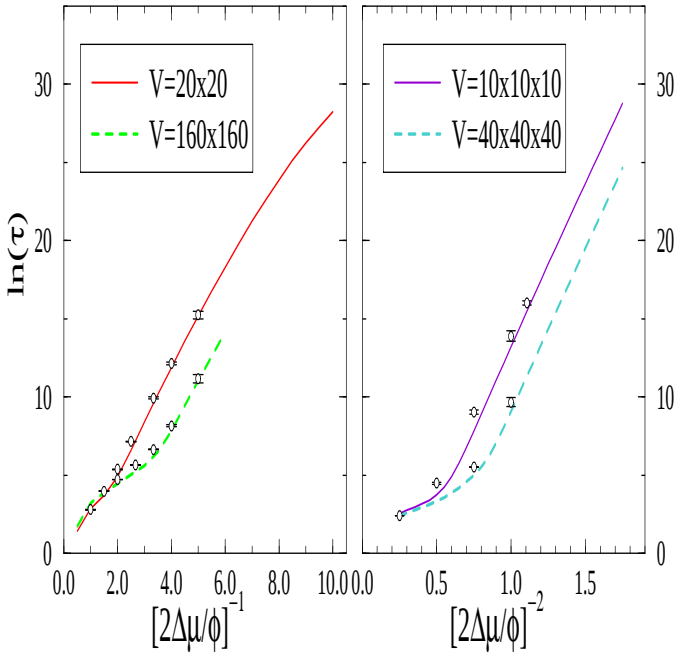

Figure 2: The average lifetime of the metastable phase, measured in MCSS, shown vs $(\phi/2|\Delta\mu|)^{d-1}$ for different system sizes and dimensions. In both parts, the curve for the smaller system is solid and the curve for the larger system is dotted. For d=2 (a), the system sizes shown are 20^2 and 160^2 at T=0.325ϕ=$0.57T_c$. For d=3 (b), the system sizes shown are 10^3 and 40^3 at T=0.5ϕ=$0.44T_c$. The symbols are from actual simulations. The curves are PD extrapolations based on equilibrium data sampled for the smaller system size. See the text for further detail. The different slopes in the MD and SD regimes are clearly seen. After Ref. [8] with additional data.

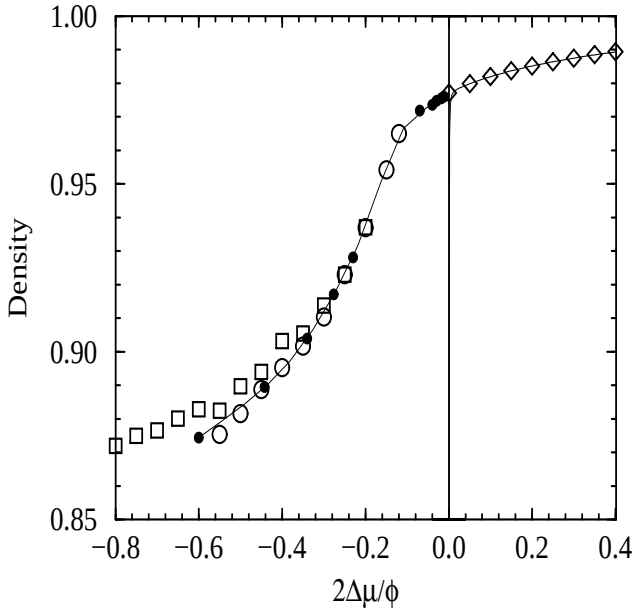

Figure 3: Metastable and stable densities for d=2 at $0.8T_c$. The equilibrium density, $\theta_{\rm s}(\Delta\mu, T)$, is shown for $\Delta\mu \geq 0$. The data points represented by empty diamonds were obtained from equilibrium MC simulations with L=256, while the thin solid curve is from a transfer-matrix calculation with strip width N=9. The metastable density, $\theta_{\rm ms}(\Delta\mu, T)$ is shown for $\Delta\mu < 0$. The data points represented by empty circles and squares were obtained by fitting MC data for $\langle\theta(t)\rangle$ to Eq. (9) as described in the text, while the filled circles represent transfer-matrix calculations with N between 5 and 9. The thin solid curve connecting the latter points is a guide to the eye only. Statistical uncertainties in the MC results are everywhere smaller than the symbol size. After Ref. [21].

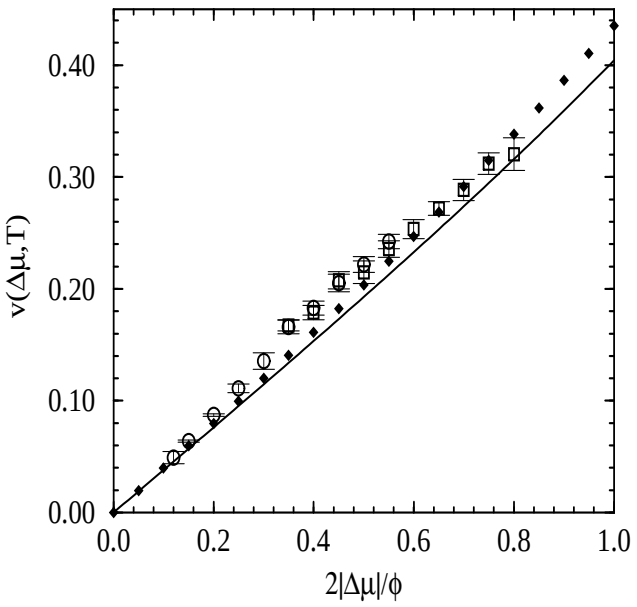

Figure 4: The average propagation velocity of the interface separating the regions of metastable and stable phase for d=2 at $0.8T_c$. The empty squares and circles represent estimates based on Eqs. (9) and (10) as described in the text. The error bars indicate the statistical uncertainties. The filled diamonds were obtained from MC simulations of a flat interface of length 1000, propagating into a region of metastable phase in which nucleation was suppressed [26]. The solid curve is an analytic nonlinear-response approximation [21, 26]. After Ref. [21] with additional data.